cal deg$^{-1}$ mole$^{-1}$, or very nearly equal to $R\ln 2 = 1.38$ cal deg$^{-1}$ mole$^{-1}$, the value for random orientation of the nuclear spins. If the reasonable assumption is made that the contribution of phonon excitation to the total entropy is small at this temperature, it can be concluded that the nuclear spins are not appreciably ordered in liquid He$^3$ at 0.42°K, in agreement with our previous prediction.[6] The results also indicate, contrary to suggestions by others,[7–9] that liquid He$^3$ cannot be treated as an ideal Fermi-Dirac gas having the same molecular weight and density as liquid He$^3$; for the entropy of such a gas at 0.42°K would be 0.84 cal deg$^{-1}$ mole$^{-1}$, instead of the measured value of $1.35\pm0.15$ cal deg$^{-1}$ mole$^{-1}$.

The present results may also be combined with data on the melting pressure to obtain the entropy of solid He$^3$. It has been been found[10] that the slope of the melting pressure curve becomes zero near 0.42°K, and hence from the thermodynamic relation,

$$dp/dT = \Delta S/\Delta V, \tag{3}$$

the difference in entropy between the compressed liquid and the solid becomes zero near this temperature. Provided that the entropy change on compression of the liquid is small, the entropy of solid He$^3$ at 0.42°K must therefore be $1.35\pm0.15$ cal deg$^{-1}$ mole$^{-1}$, which corresponds to random orientation of the nuclear spins in the solid. This conclusion substantiates Pomeranchuk's assumption[11] regarding nuclear spin alignment in solid He$^3$.

[1] J. Kistemaker, Physica **12**, 272, 281 (1946).
[2] H. van Dijk and D. Shoenberg, Nature **164**, 151 (1949).
[3] C. F. Squire, *Low Temperature Physics* (McGraw-Hill Book Company, Inc., New York, 1953), p. 233.
[4] A. H. Cooke, Proc. Phys. Soc. (London) **A62**, 269 (1949).
[5] Abraham, Osborne, and Weinstock, Phys. Rev. **80**, 366 (1950).
[6] Weinstock, Abraham, and Osborne, Phys. Rev. **89**, 787 (1953).
[7] E. M. Lifshitz, J. Exptl. Theoret. Phys. (U.S.S.R.) **21**, 659 (1951).
[8] K. S. Singwi, Phys. Rev. **87**, 540 (1952).
[9] T. C. Chen and F. London, Phys. Rev. **89**, 1038 (1953).
[10] Weinstock, Abraham, and Osborne, Phys. Rev. **85**, 158 (1952), and unpublished results.
[11] I. Pomeranchuk, J. Exptl. Theoret. Phys. (U.S.S.R.) **20**, 919 (1950).

## Energy Loss of Electrons in Passage Through Thin Films*

L. MARTON AND LEWIS B. LEDER
*National Bureau of Standards, Washington, D. C.*
(Received February 8, 1954)

THIS is a preliminary report on measurements of the energy loss spectrum of 30-kev electrons passing through thin films of metals and insulators. These losses are of the same type as those measured by Ruthemann,[1] Lang,[2] and Möllenstedt,[3] and as those calculated by Pines and Bohm[4] by means of their "plasma oscillation" theory of metals.

To make these measurements, we modified an electrostatic electron microscope by replacing its two projection lenses with a slit and a "cylindrical" lens. The analysis of the scattered primary beam is accomplished by utilizing the off-axis chromatic aberration of the "cylindrical" lens.[5] The slit has a fixed spacing of approximately 2 microns, and was built into the shell of one of the projection lenses with provision made for rotation and translation from outside the vacuum of the instrument. The "cylindrical" lens was made using the shell and outer electrodes of the other projection lens, and replacing the center electrode by an element with an elongated aperture. These were placed in the former projection lens positions with the slit above the lens. After proper alignment, as described by Möllenstedt, it was found that the projected image of the slit could be shifted parallel to itself when the accelerating potential was changed relative to the lenses. With this arrangement we have obtained an energy resolution of 1 part in 35 000.

The thin films, which were between 50 and 100A thick, were prepared by evaporation onto salt crystal faces, floated off on water, and mounted on 200-mesh screens. These were placed in the normal object position of the microscope so that an enlarged image appeared on the slit. In cases where the material oxidized rapidly in the air, it was evaporated onto another thin film substrate in the vacuum of the analyzer itself.

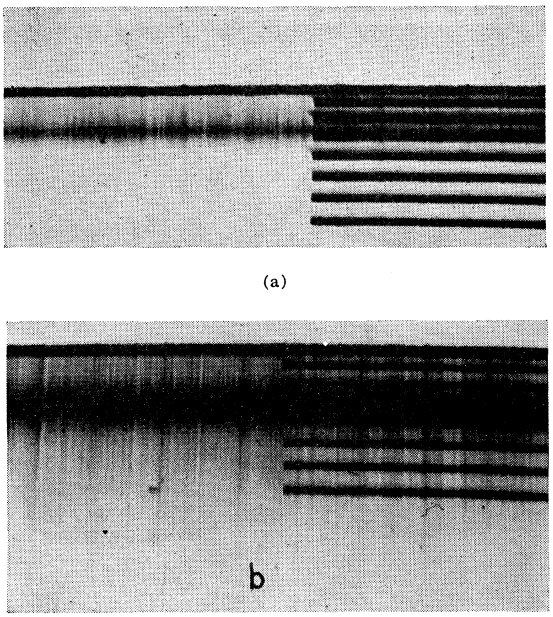


(a)

(b)

FIG. 1. Examples of the type of spectra obtained. Fig. 1(a) is the spectrum of germanium, and Fig. 1(b) is the spectrum of beryllium. The top line in each case represents the primary energy. The diffuse line on the left is the energy spectrum of electrons transmitted through the scatterer, and on the right are calibration markers spaced 6 ev apart.

Figure 1 shows examples of the type of spectra obtained. On the left is the energy spectrum of electrons transmitted through the film, and on the right are calibration markers spaced 6 ev apart. The spectrum contains, besides the undisturbed baseline, one or more lines which in some cases are quite sharp. Table I lists preliminary values of the energy losses corresponding to the maxima of these lines for the materials which we have measured so far. The letters *a*, *b*, *c*, *d*, and *e* shown as subscripts to the

TABLE I. Energy loss values in ev for approximately 30-kev electrons passing through thin films of various materials. The subscripts refer to estimated widths of the lines (see text).

| Material | Energy loss values in ev |
|---|---|
| Beryllium | $6.5_a$ $18.9_e$ |
| Na on quartz | $5.4_a$ $10.7_a$ $13.3_a$ $17.5_c$ |
| Na on collodion | $5.1_a$ $10.8_a$ $17.5_b$ $18.6_c$ |
| Magnesium | $9.7_a$ $20.3_d$ |
| Aluminum | $6.2_a$ $13.9_a$ $19.2_b$ $27.8_a$ $35.0_b$ |
| Silicon | $5.2_a$ $16.9_c$ |
| K on silicon | $7.8_a$ $11.3_a$ $15.0_a$ $18.7_a$ $22.6_a$ $27.8_b$ |
| K on collodion | $8.0_a$ $11.0_a$ $14.9_a$ $19.5_a$ $22.7_a$ $25.8_b$ |
| Titanium | $11.4_a$ $21.4_b$ $42.9_b$ |
| Chromium | $9.7_a$ $21.8_d$ 45.0 |
| Manganese | $9.9_a$ $22.1_d$ |
| Iron | $15.8_b$ $19.4_b$ 56.1 |
| Cobalt | $5.7_a$ $18.3_c$ |
| Nickel | $5.8_a$ $9.4_a$ $13.2_a$ $17.6_c$ $23.4_c$ |
| Copper | $6.9_a$ $11.3_a$ $19.6_d$ |
| Germanium | $16.0_b$ $30.1_b$ |
| Palladium | $15.7_a$ $21.5_a$ |
| Silver | $16.0_c$ |
| Cadmium | $14.5_a$ |
| Tin | $4.5_a$ $12.4_a$ $18.0_a$ $23.9_a$ |
| Antimony | $14.2_a$ $24.3_a$ |
| Gold | $16.5_a$ $21.5_a$ |
| Bismuth | $13.0_a$ $25.2_a$ |
| Collodion | $4.5_a$ $19.3_d$ |
| Quartz | $5.5_a$ $19.4_e$ |
| Air (nitrogen) | $12.9_a$ |

energy-loss values denote the estimated relative "half-widths" of the loss distribution. *a* indicates an estimated "half-width" equal to the unscattered slit image (approximately 1.2 volts), *b* a width twice *a*, *c* three times, etc. Figure 1(a) shows the scattering in germanium and is an example of an *a*-type distribution, while Fig. 1(b) shows the scattering in beryllium which is an example of the *e*-type distribution. Where previous measurements have been made, the extent of agreement varies.

In most cases more than one line has been observed. Where higher values appear to be multiples of some lower one, this would indicate repeated occurrence of the same event. Where the higher values are not multiples of some lower one, it may be an indication that not only lattice interaction but also atomic interaction may be responsible for the observed spectrum. In particular, the highest values for chromium and iron can perhaps be identified with the $M_{II}M_{III}$ x-ray absorption values while the single value found for cadmium is close to its $N_{IV}$ x-ray absorption value.

Pines and Bohm[4] have calculated some values of energy loss by means of their plasma oscillation theory. They give 15.9 ev for aluminum and 18.8 ev for beryllium. Also, Pines[5] has calculated 10.8 ev for magnesium and ~6 ev for sodium. These values are in reasonable agreement with our measured ones. In a recent paper Wolff[6] has stated that one would expect the widths of the absorption peaks to increase from element to element in the transition series, Sc through Ni, as the *3d* shell is filled. Our estimated band widths indicate that this may not be the case. However, further careful analysis of the bands is necessary before this can be stated more definitely. Similar losses have also been observed by Rudberg,[7] Haworth,[8] Turnbull and Farnsworth,[9] and Reichertz and Farnsworth[10] by measuring the energy distribution of very low-energy electrons reflected from metallic surfaces. It is highly probable that these were due to the same mechanism as the losses observed in transmission.

* This work was supported by the U. S. Office of Naval Research.
[1] G. Ruthemann, Naturwiss. **29**, 648 (1941); Ann. Physik **2**, 113 (1948).
[2] W. Lang, Optik **3**, 233 (1948).
[3] G. Möllenstedt, Optik **5**, 499 (1949); Zeit. angew. Phys. **3**, 187 (1951); Optik **9**, 473 (1952).
[4] D. Pines and D. Bohm, Phys. Rev. **85**, 338 (1952); D. Pines, Phys. Rev. **92**, 626 (1953).
[5] D. Pines (private communication).
[6] P. A. Wolff, Phys. Rev. **92**, 18 (1953).
[7] E. Rudberg, Kgl. Svenska Vetenskapsakad. Handl. **7**, 1 (1929); Proc. Roy. Soc. (London) **A127**, 111 (1930); Phys. Rev. **50**, 138 (1936).
[8] L. J. Haworth, Phys. Rev. **37**, 93 (1931); **42**, 906 (1932); **48**, 88 (1935).
[9] J. C. Turnbull and H. E. Farnsworth, Phys. Rev. **54**, 509 (1938).
[10] P. P. Reichertz and H. E. Farnsworth, Phys. Rev. **75**, 1902 (1949).

## Coulomb Excitation by Means of Bombardment with Various Particles

JØRGEN H. BJERREGAARD AND TORBEN HUUS
*Institute for Theoretical Physics, University of Copenhagen, Copenhagen, Denmark*
(Received February 10, 1954)

THE production of Coulomb excitation effects by the impact of different types of projectiles, such as protons, deuterons, and $\alpha$ particles, not only gives a very convincing check on the nature of the process, but also provides a simple method for determining the multipole order of the transition in question.[1]

The cross section for Coulomb excitation produced by the electric multipole field of order $\lambda$ of the impinging particle may be written[2]

$$\sigma = Z_1^2 \frac{B_e(\lambda)}{e^2 a^{2\lambda}} \cdot \left(\frac{a}{v}\frac{e^2}{\hbar}\right)^2 \cdot f_\lambda\{\xi\}, \tag{1}$$

where

$$a = \frac{Z_1 Z_2 e^2}{mv^2}; \quad \xi = \frac{Z_1 Z_2 e^2 \Delta E}{\hbar m v^3}. \tag{2}$$

Here $Z_1 e$ is the charge, $m$ the reduced mass, and $v$ the velocity of the bombarding particle, whereas $Z_2 e$ is the charge, $\Delta E$ the excitation energy, and $B_e(\lambda)$ the reduced transition probability[3] for the target nuclei. The function $f_\lambda\{\xi\}$ has been evaluated for the case $\lambda=2$ by Alder and Winther.[4] The expression (1), which can be deduced from simple dimensional arguments, is derived by considering the projectile as moving along its classical trajectory, and neglecting the change in the orbit caused by the energy loss $\Delta E$.

Elimination of $a$ and $v$ from (1) and (2) gives

$$\sigma = C_\lambda\{Z_2, \Delta E, B\} Z_1^2 \left(\frac{m}{Z_1}\right)^{2\lambda/3} \xi^{2-4\lambda/3} f_\lambda\{\xi\}, \tag{3}$$

where $C_\lambda$ is a constant which depends only on $\lambda$ and the properties of the target nuclei.

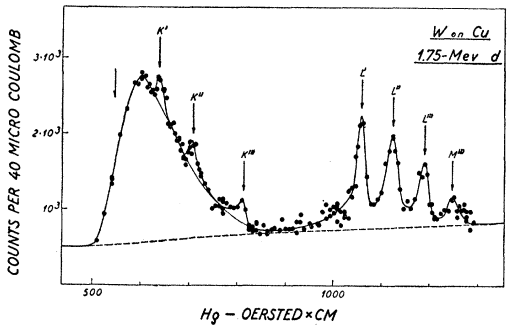


FIG. 1. The $\beta$ spectrum measured for W bombarded by 1.75-Mev deuterons. The cutoff at small momenta is due to the 0.9-mg/cm² mica window of the counter. The dashed line indicates the general background mainly due to the effect of penetrating radiation from carbon deposits.

One can thus directly determine the multipole order of the excitation process by comparing, for the same value of $\xi$, the cross sections obtained with particles having different $m/Z_1$ ratios.

We have tested these conclusions by means of measurements on W bombarded with protons, deuterons, and $\alpha$ particles in the energy range from 1 to 2 Mev.[5] Figure 1 shows the entire $\beta$ spectrum obtained by bombardment with 1.75-Mev deuterons. For the present purpose we used mainly the $L'$ peak, which corresponds to an excitation energy of 100 kev assigned to the first excited state in $W^{182}$.[6]

When the background is subtracted, the peak height $y$ of the line can be used as a measure of the corresponding cross section, since the thickness of the target layer was only about $\frac{1}{2}$ mg/cm². Figure 2 shows a plot of $\log_{10}(y/Z_1^2)$ *versus* $\xi$. The points for deuterons and $\alpha$ particles should be shifted a constant amount

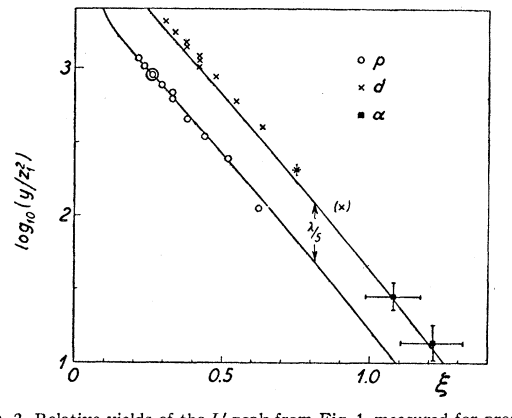


FIG. 2. Relative yields of the $L'$ peak from Fig. 1, measured for protons, deuterons, and $\alpha$ particles of energies between 1 and 2 Mev. The constant distance $\lambda/5$ shows the multipole order of the excitation process. The theoretical curves for $E2$ excitation are normalized at the point marked with a ring. The $\xi$ values have been corrected for the effect of the target thickness, but not for the energy $\Delta E$ lost by the excitation.

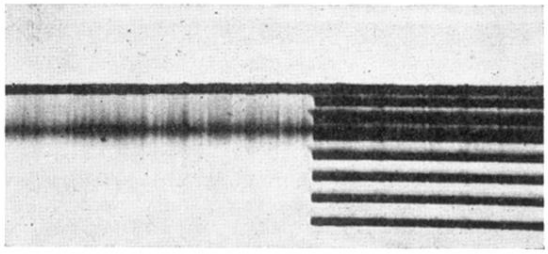

(a)

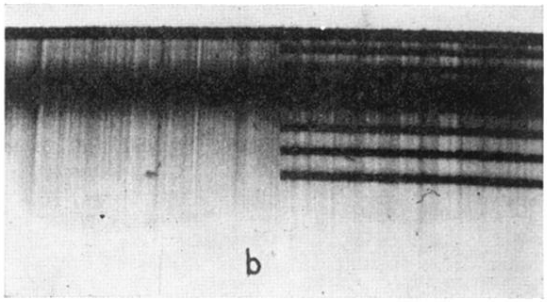


(b)

FIG. 1. Examples of the type of spectra obtained. Fig. 1(a) is the spectrum of germanium, and Fig. 1(b) is the spectrum of beryllium. The top line in each case represents the primary energy. The diffuse line on the left is the energy spectrum of electrons transmitted through the scatterer, and on the right are calibration markers spaced 6 ev apart.